

Research on wooden window nodes of optimal design

Jing Liu¹, Yingqi Chen¹, Fei Meng¹, and Zongxue Chen²

¹College of Civil Engineering and Architecture, Hebei University, Baoding, Hebei, 071002, China

²Hebei construction group corporation limited, Baoding, Hebei, 071052, China

Abstract. Mortise connection is a unique way of connection in the wood structure of ancient buildings in China. This paper takes the mortise and mortise joints of wood window frame as the object. Eight models of wooden window frames are built in ANSYS software with the parameters of tenon diameter and tenon length. The static performance of them is studied. Through simulation loading, the ultimate bearing capacity of the model under vertical and horizontal loads is obtained, and it is concluded that the Mohr strength of the dangerous point and the maximum displacement value at the contact of the mullion and mullion are linearly related to the applied load. Through the parameter analysis, such as the diameter and length of mortise and tenon joint, the optimal design of this kind of mortise and tenon joint component are carried out so as to provide the theoretical basis for its application in the actual project.

1.Introduction

Mortise and tenon structure is a kind of component which combines the concave and convex parts to connect the two components[1]. The protruding part is tenon, the concave part is mortise. This unique connection mode endows the wood structure with good elasticity, and each node is rigid and flexible, which makes the wood structure have good energy consumption capacity. Therefore, this kind of connection structure is widely used in ancient wood structure buildings in China, and it is still used in the design and manufacture of modern wood furniture and prefabricated wooden villa[2].

The mechanical mechanism of mortise and mortise structural connections are very complex. During the processing, the section of mortise and mortise joint will be weakened, the bearing capacity will be reduced, and it is easy to become the weak part in the structure[3]. There are more than 100 kinds of mortise and mortise structures, which can be roughly divided into face to face structure, point structure, and joint mortise and mortise structures. In this paper, it is studied that the static performance analysis of face to face mortise and tenon structure under vertical and horizontal loads.

2. Establishment of finite element model

In this paper, the finite element model is built in ANSYS software according to the dimension of the solid model of wooden window frame provided. Because the model is axisymmetric, in order to simplify the calculation, one half of the whole model can be built in the software. The wood window frame model are shown in Fig.1—Fig.4.

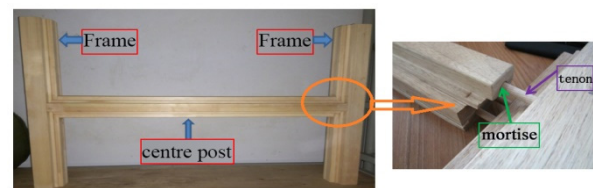


Fig.1. Entity model

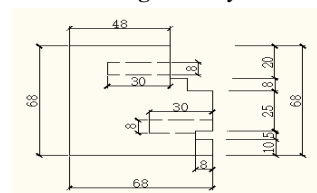


Fig.2. Sectional dimension of mullion

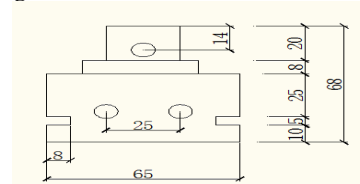


Fig.3. Cross section dimension of cross stiles

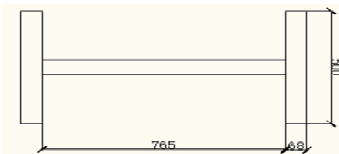


Fig.4. Dimensional drawing of solid model

In the selection of wood window frame materials, the imported wood pineapple material is selected according to the stress analysis and strength checking calculation of bucket arch joint area, with the density of 800kg/m^3 and the friction coefficient of 0.2. In the calculation, nine

independent elastic constants are defined, which are respectively the elastic modulus E_1, E_2, E_3 , Poisson's ratio $P_{RX-Y}, P_{RX-Z}, P_{RY-Z}$, shear modulus G_X, G_Y, G_Z in three directions, as shown in Table 1. The compressive strength f_c , the tensile strength f_t , the shear strength f_v , the bending strength f_m and the transverse compressive strength f_{c-90} of the wood are defined respectively. The specific values are shown in Table 2.

Table 1 The parameters of wood mode

E_1	E_2	E_3	P_{RX-Y}	P_{RX-Z}	P_{RY-Z}	G_X	G_Y	G_Z
12.2×10^9	12.2×10^9	12.2×10^9	0.1	0.1	0.1	6.1×10^8	6.1×10^8	6.1×10^8

Table 2 Wood strength (unit: MPa)

f_c	f_t	f_v	f_m	f_{c-90}
18	12	2.8	20	4.2

To control the diameter and length of different mortise and tenon, 8 models of mortise and tenon structures are established, and the detailed dimensions are shown in Table 3.

Table 3 The dimensions of mortise and tenon (unit: mm)

Model number	D7	D8a	D8b	D9	D10a	D10b	D12a	D12b
Tenon diameter	7	8	8	9	10	10	12	12
Tenon length	60	60	80	60	60	80	60	80

According to the analysis of the concrete situation of wooden frame mortise and tenon structure, solid element solid45, which can simulate the actual working performance of the joint of mullion and mullion in the wooden window frame, is selected to simulate. Compared with the direct modeling method, the more general solid modeling method is used in the modeling method. During the establishment, the overall coordinate system is used for the cross mullion and mullion, and the local coordinate system is used for the round bar. In order to improve the quality of grid division, the image division method is used to make the grid division in the contact part of mullion and mullion more precise, and the grid division in other parts can be slightly rough.

In this model, the target surface is the surface of the round bar, the contact surface is the inner surface of the cross bar and the groove of the mullion that contact with the round bar, and the contact surface between the cross bar and the mullion is the target surface, and the contact surface between the cross bar and the mullion that contact with the mullion defines four contact pairs. For the analysis of contact problems, the important factor affecting the calculation accuracy and convergence is the contact stiffness[4], which needs to be selected through some relevant experience. For large-area solid contact, we can estimate the normal contact stiffness factor $FNK = 1.0$; for the soft part (bending dominates), we can estimate $FNK = 0.01 \sim 0.1$. The normal contact stiffness factor of this model is 0.01.

Finally, the constraints of boundary conditions are consistent with the actual situation of the model, and symmetrical constraints are applied on the middle surface of the mullion. The upper end of mullion constrains the displacement in X, Y direction, and the free sliding in Z direction. The lower end of the mullion constrains the displacement in X, Y and Z directions.

3. Simulation analysis

In the way of loading, the vertical load and the horizontal load are explored. Under the vertical load, toughened glass is selected as the wood window glass, with a density of $2500 \text{kg} / \text{m}^3$ and a thickness of 5mm. The gravity of 1 m high tempered glass is converted into line load of 0.125KN/m. The weight of toughened glass of different height can be converted into line load according to the weight of toughened glass of 1m height. In the experiment, the weight of glass can be converted into surface load and added to the groove surface of glass and mullion contact. Under the action of horizontal load, when the wind load acts on the wooden window, its stress direction is perpendicular to the plane of the wooden window, and the load-bearing unit composed of the wooden window frame can be regarded as the simply supported plate hinged on four sides. The distribution of wind load can be simplified as trapezoid or triangle. The horizontal wind load is applied to the surface of the mullion and the mullion, and the reduced surface load is applied to the groove where the glass and the mullion contact with the mullion.

3.1 Research on ultimate bearing capacity

In the experiment, D10a model is taken as an example, which is loaded vertically first to explore the selection of strength theory and study the stress state. The first principal stress, the second principal stress and the third principal stress at the most dangerous point should be checked, and the strength value according to the Mohr strength theory and the double shear stress strength theory [5] should be calculated, as shown in Table 4. Mohr's strength and double shear strength at different glass heights of D10a model it can be seen from the chart that the calculation results of nodes under Mohr's strength theory are greater than those under double shear strength theory, so we can think that the control strength condition of dangerous points of the model is Mohr's strength theory, so this experiment is based on Mohr's strength theory.

Table 4 Mohr strength and double shear strength of different glass heights of D10a model

Glass height (m)	Line load (N/m)	First principal stress σ_1 (MPa)	Second principal stress σ_2 (MPa)	Third principal stress σ_3 (MPa)	Molar principal stress σ_{M} (MPa)	Double shear stress strength σ_{d2} (MPa)
0.50	62.50	2.4891	1.5249	-1.0707	3.2029	2.2598
1.00	125.00	3.6171	2.4678	-1.1572	4.3886	2.9618
1.50	187.50	5.0782	3.0877	-1.0691	5.7909	4.0689
2.00	250.00	6.6361	3.6064	-0.99419	7.2989	5.3300
2.50	312.50	8.2164	4.13	-0.93885	8.8423	6.6208
3.00	375.00	9.809	4.6793	-0.92367	10.4248	7.9312
3.50	437.50	11.413	5.2951	-0.98935	12.0726	9.2601

The relationship between Mohr strength of the most dangerous point and glass height of D10a model is shown in Fig.5. In the case of vertical load, through the Mohr strength theory calculation, when the glass height is 3.0m, $\sigma_M = 10.4248 \text{MPa} < [\sigma] = 12 / 1.1 = 10.91 \text{MPa}$, when the glass height is 3.5m, $\sigma_M = 12.0726 \text{MPa} > [\sigma]$, it can be seen that the ultimate bearing capacity of the model is between 3.0 ~ 3.5m. Mohr strength increases linearly

with the increase of glass height, and the more accurate glass height corresponding to the ultimate bearing capacity can be calculated by interpolation as 3.15m..

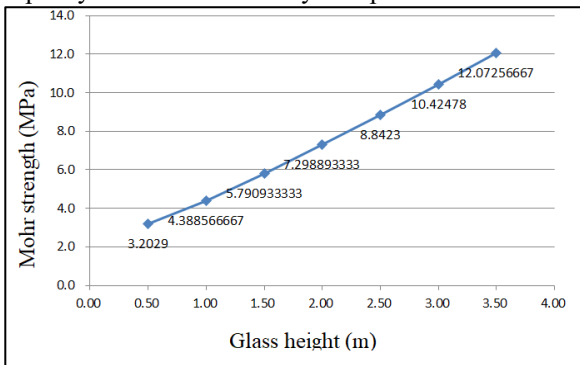


Fig.5.Relationship between Mohr strength of the most dangerous point and glass height of D10a model.

The same experimental method is used to test the components under horizontal load. When different horizontal loads are applied, the stress state and strength checking calculation of dangerous points in D10a model is shown in Fig.6.

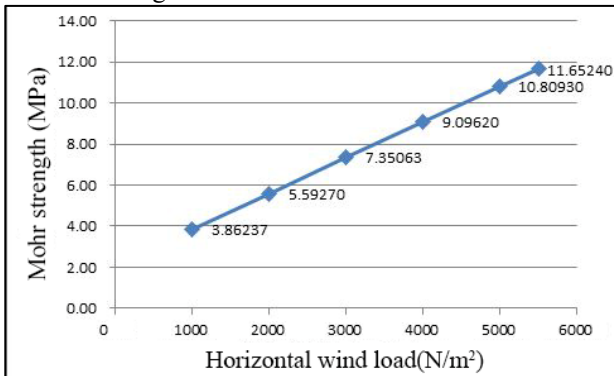


Fig.6.The relationship between the horizontal load on different glass and the Mohr strength at the most dangerous point

3.2 Displacement value at the contact of model mullion and mullion and in the span

Under the action of vertical load, it is found that there are cracks in the contact part between the mullion and the mullion. By looking at the displacement nephogram of the contact part of the mullion, it is found that the cracks increase with the increase of load. Through the analysis of specific data, the displacement value under vertical load increases linearly with the increase of load, as shown in Figure 7. The maximum displacement and mid span deflection at the contact part of the cross and mullion are shown in Table 5 .

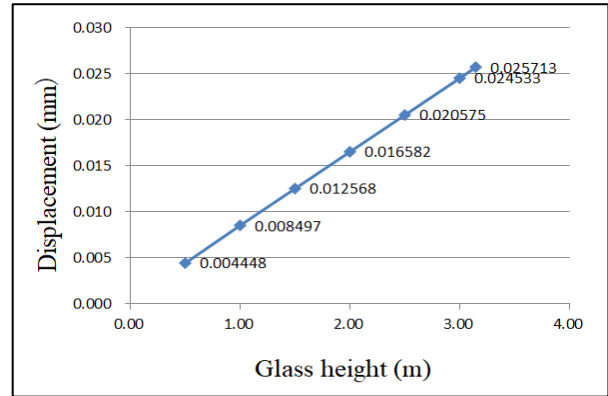


Fig.7.The relationship between the glass height and the maximum displacement in D10a model

Table 5 Displacement value for each model reaching the ultimate bearing capacity

Model number	D7	D8a	D8b	D9	D10a	D10b	D12a	D12b
Maximum displacement (mm)	0.0249	0.0203	0.0336	0.0195	0.0257	0.0267	0.0258	0.0264
Midspan deflection (mm)	0.155	0.145	0.186	0.132	0.17	0.176	0.167	0.179

When the horizontal load is applied, the failure also occurs at the contact part of cross and mullion. Through specific data analysis, the displacement value increases linearly with the load, as shown in Fig. 8. The maximum displacement and mid span deflection at the contact part of the cross and mullion are shown in Table 6 .

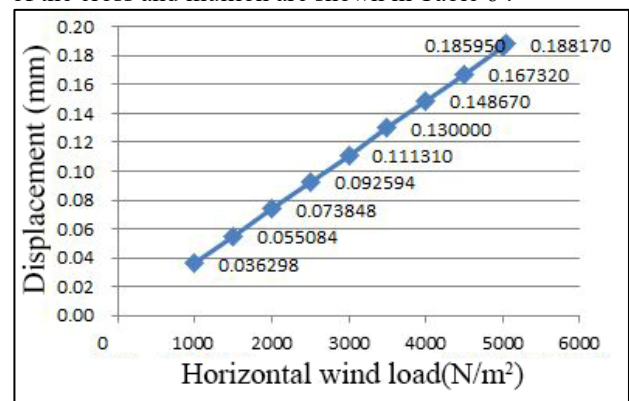


Fig.8.The relationship between the maximum displacement and the horizontal wind loads on the D10a model

Table 6 Displacement value while each model reaching the ultimate bearing capacity

Model number	D7	D8a	D8b	D9	D10a	D10b	D12a	D12b
Maximum displacement (mm)	0.1738	0.1448	0.1395	0.1817	0.1882	0.1667	0.2208	0.2356
Midspan deflection (mm)	0.954	0.793	0.6	0.985	1.035	0.646	1.216	1.195

According to the code for design of timber structures [6], the allowable deflection value of this component $[\omega] = L / 250 = 765\text{mm} / 250 = 3.06\text{mm}$, and the calculated mid span deflection values are less than the allowable deflection values, so it meets the relevant requirements.

According to the code for design of timber structures [6], the allowable deflection value of this component $[\omega] = L / 250 = 765\text{mm} / 250 = 3.06\text{mm}$, and the calculated mid span deflection values are less than the allowable deflection values, so it meets the relevant requirements.

3.3 Simulation conclusion analysis

In the vertical load, compared with five models with tenon length of 60mm, it is found that the ultimate bearing capacity is larger when the diameter is 10 mm.

Compared with the model with the diameter of the tenon of 16mm, it can be seen that the larger the diameter of the tenon, the greater the ultimate bearing capacity. Compared with 6 models with 8,10,12mm diameter, it is found that when the diameter of tenon is fixed, increasing the length of tenon will improve the ultimate bearing capacity of the joint, and the model with 8mm diameter of tenon will increase the most obviously. Compared with all models, the maximum vertical ultimate bearing capacity is D10b model. The comparison Fig. is shown in Fig. 9 and Fig. 10.

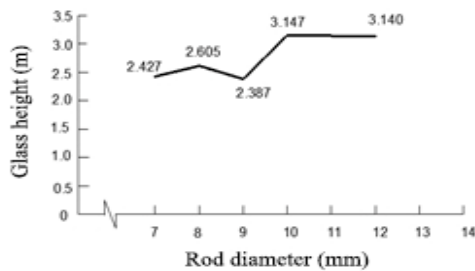


Fig.9. Comparison of height of glass with different tenon diameter and same tenon length

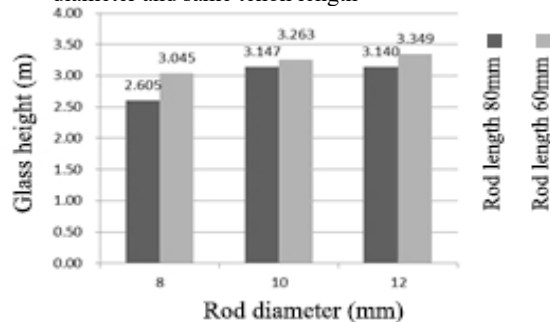


Fig.10. Comparison of glass height with the same tenon diameter and different tenon length

Compared with the five models with a tenon length of 60mm, it is found that the ultimate bearing capacity is the largest when the tenon diameter is 12mm. The ultimate bearing capacity tends to increase with the diameter, but it is not that the larger the diameter is, the larger the ultimate bearing capacity is. When the diameter of the tenon is 16mm and the horizontal load is 1000N /m², the material has been damaged, and the maximum Mohr strength reaches 13.261mpa. When the length of tenon is increased, it is found that the ultimate bearing capacity of the model with diameter of 8mm and 10 mm is decreased, while that of the model with diameter of 10 mm is increased. Therefore, the D12b model has the largest ultimate bearing capacity. The comparison Fig. is shown in Fig. 11 and Fig. 12:

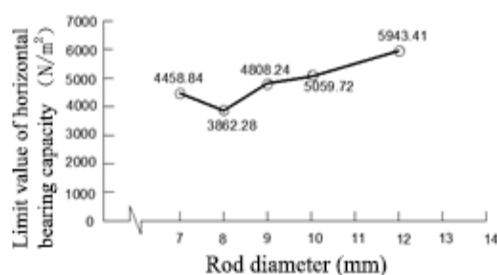


Fig.11. Comparison of ultimate horizontal bearing capacity of different tenons with the same diameter and tenon length

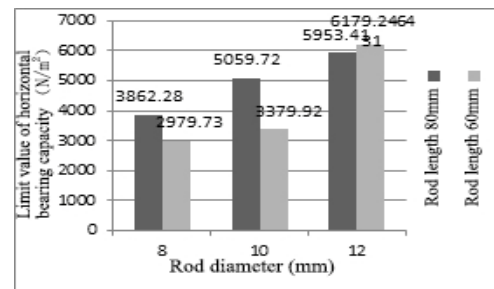


Fig.12. Comparison of ultimate horizontal bearing capacity of different tenon lengths with the same tenon diameter

4.The conclusion

Considering the vertical load and the stress-strain situation under the horizontal load, considering the size requirements of the wooden window and the size deviation during the processing, the paper makes a comprehensive comparative analysis of eight models, and draws the following conclusions:

The model with the largest ultimate bearing capacity of this kind of wooden window is the model with a tenon diameter of 10 mm and a tenon length of 60 mm. Under the vertical load, it can bear a maximum line load of 393.38 N / m, a maximum displacement value of 0.0257 mm at the contact part between the crossbeam and the mullion, a maximum wind load of 5059.72 N / m² under the horizontal load, and a maximum displacement value of 0.1882 mm at the contact part between the crossbeam and the mullion.

Acknowledgement

Supported by Natural Science Foundation of Hebei Province(E2017201158), "one province, one university" special fund, Foundation of Hebei Educational Committee(QN2016171). Innovation and entrepreneurship project of Hebei University.

References

1. G.F.Wu, Y.Zhong, Y.C.Gong, H.Q.Ren, China wood industry.J. *E* **33**,25 (2019)
2. S.Y.Shen,W.Xu., Art Science and Technology .J *The present situation and trend of folding wood furniture with wood cutting structure. Art technology* (2019)
3. J.X.Wang, *Static and dynamic analysis of mortise mortise joint wood structure* .D. (Kunming University of technology, 2008)
4. M.H.Yu, Y.J.Peng, Progress in mechanics.J. *century's summary of strength theory* (2004)
5. X.F.Sun, X.F.Fang,L.T.Guan, Beijing: Higher Education Press. *Materials Mechanics (I)*(2010)
6. National standard of the people's Republic of China. Gb50005-2003. *Code for design of timber structures*.S. (Beijing: China Building Industry Press, 2003)